

Table II shows the results of recent computer simulations for the xenon self-diffusion in ZSM-5. It is remarkable that both the absolute values and the predicted concentration dependence are in reasonable agreement with the NMR data.

### Conclusion

$^{129}\text{Xe}$  NMR has been successfully applied to study the self-diffusion of xenon in zeolites. The measurement of the mean-square displacement in dependence on the observation time yielded a linear relation as required for ordinary, intracrystalline self-diffusion. In zeolites NaX and ZSM-5, the self-diffusion coefficients were found to decrease with increasing concentration while

for zeolite NaCaA they are essentially constant. The highest diffusivities were observed in zeolite NaX. This is in agreement with the fact that due to the internal pore structure the steric restrictions of molecular propagation in zeolite NaX are smaller than those in NaCaA and ZSM-5.

For zeolite NaCaA the obtained diffusivities are by several orders of magnitude larger than literature data based on both uptake experiments and computer simulation. Recent computer simulations of xenon diffusion in ZSM-5, however, are found to be in satisfactory agreement.

Registry No. Xe, 7440-63-3.

## Two-Dimensional NMR Studies of Native Coenzyme F430

Hoshik Won,<sup>†</sup> Karl D. Olson,<sup>‡</sup> Ralph S. Wolfe,<sup>\*,‡</sup> and Michael F. Summers<sup>\*,†</sup>

Contribution from the Department of Chemistry and Biochemistry, University of Maryland Baltimore County, Baltimore, Maryland 21228, and Department of Microbiology, University of Illinois at Urbana-Champaign, Urbana, Illinois 61801. Received August 4, 1989

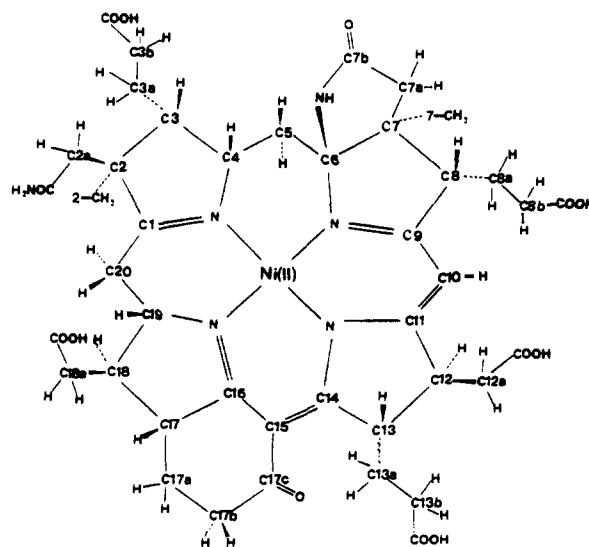
**Abstract:** Modern two-dimensional (2D) NMR spectroscopic methods are used to determine signal assignments and structural features of the recently discovered nickel(II)-containing coenzyme F430. This is the first detailed  $^1\text{H}$  and  $^{13}\text{C}$  NMR study of the native form of coenzyme F430. With the use of COSY, HOHAHA, NOESY, and ROESY  $^1\text{H}$ - $^1\text{H}$  correlated spectroscopies in combination with HMQC and HMBC  $^1\text{H}$ - $^{13}\text{C}$  correlated spectroscopies, signal assignments were made for all carbon atoms and nonexchangeable protons. The data confirm 16 of the 21 specific  $^{13}\text{C}$  NMR signal assignments made earlier for native F430 by classical 1D NMR methods and provide assignment (or reassignment) of the remaining carbon atoms. The  $^1\text{H}$  NMR signal assignments reported here are in good agreement with the partial assignments reported previously for the pentamethyl ester derivative of F430 (F430M) in  $\text{CD}_2\text{Cl}_2$  solution. In addition, long-range through-bond  $^1\text{H}$ - $^{13}\text{C}$  connectivities confirm aspects of the F430 structure deduced from studies of F430M by traditional spectroscopic and chemical methods.

Coenzyme F430, discovered just over 10 years ago, is a nickel-containing cofactor for methyl-coenzyme M reductase that is produced in methanogenic bacteria.<sup>1-4</sup> By an unknown mechanism, F430 mediates the reductive demethylation of methyl-coenzyme M (2-(methylthio)ethanesulfonic acid,  $\text{CH}_3\text{-S-CoM}$ ) using reducing equivalents from (7-mercaptoheptanoyl)threonine phosphate (HS-HTP), producing methane and the heterodisulfide of methyl-coenzyme M and HS-HTP ( $\text{CoM-S-S-HTP}$ ).<sup>5,6</sup> This is the last step in the conversion of  $\text{CO}_2$  to methane in what is believed to be an energy-yielding process in methanogens.

Although single-crystal X-ray data are not available, structural features of F430 have been deduced from extensive chemical and spectroscopic studies of the pentamethyl ester derivative, F430M.<sup>7-10</sup> From several biosynthetically  $^{13}\text{C}$ -labeled F430M samples and with the use of classical one-dimensional (1D) NMR experiments, specific  $^1\text{H}$  and  $^{13}\text{C}$  NMR signal assignments were made for 42 out of 46 total protons and for 21 out of 42 total carbons (excluding methyl ester carbons). Stereochemical assignments were also made for 10 of the 11 chiral corphin ring carbons in F430M. Although studies in aqueous solution were precluded by paramagnetic broadening, a partial  $^{13}\text{C}$  NMR assignment was made for the native (free acid; Chart I) form of F430 in trifluoroethanol (TFE) solution on the basis of comparisons of its 1D  $^{13}\text{C}$  NMR spectrum with the  $^{13}\text{C}$  NMR spectrum obtained for F430M.<sup>9</sup> The  $^1\text{H}$  NMR signals of native F430 in TFE solution were broadened extensively in the 300-MHz spectra and were not assigned or studied in detail.<sup>9</sup>

It has been shown that NMR signal assignments made on the basis of chemical shift analyses and other classical methods are sometimes susceptible to error.<sup>11-13</sup> With the development of new 2D NMR spectroscopic methods that provide long-range

Chart I



through-bond connectivity information, it is possible to determine unambiguously structural elements and NMR signal assignments

- (1) Gunsalus, R. P.; Wolfe, R. S. *FEMS Microbiol. Lett.* **1978**, *3*, 191.
- (2) Diekert, G.; Konheiser, U.; Piechulla, K.; Thauer, R. K. *J. Bacteriol.* **1981**, *148*, 459.
- (3) Walsh, C. T.; Orme-Johnson, W. H. *Biochemistry* **1987**, *26*, 4901.
- (4) Rouviere, P. E.; Wolfe, R. S. *J. Biol. Chem.* **1988**, *263*, 7913.
- (5) Bobik, T. A.; Olson, K. D.; Noll, K. M.; Wolfe, R. S. *Biochem. Biophys. Res. Commun.* **1987**, *149*, 455.
- (6) Ellermann, J.; Hedderich, R.; Boecher, R.; Thauer, R. K. *Eur. J. Biochem.* **1988**, *172*, 669.
- (7) Faessler, A.; Pfaltz, A.; Mueller, P. M.; Farooq, S.; Kratky, C.; Kraeutler, B.; Eschenmoser, A. *Helv. Chim. Acta* **1982**, *65*, 812.

\* To whom correspondence should be addressed.

<sup>†</sup> University of Maryland Baltimore County.

<sup>‡</sup> University of Illinois at Urbana-Champaign.

for biomolecules. Examples of these new techniques have been illustrated in recent studies of coenzyme B<sub>12</sub>.<sup>11,12</sup> Additionally, with the development of NMR-based distance geometry methodologies,<sup>14,15</sup> molecular structures can be determined to high atomic level resolution from solution-state NMR data, and this is particularly important for samples that are difficult to crystallize as is the case for F430M.<sup>8</sup> For 3D structure determination, complete assignment of the <sup>1</sup>H NMR signals is a crucial prerequisite.

We have found that the <sup>1</sup>H NMR signals of the native form of coenzyme F430, obtained using TFE-*d*<sub>3</sub> as the solvent at high magnetic field strength (11.75 T; 500 MHz), are sufficiently narrow to allow detailed investigations with recently developed 2D NMR techniques, including homonuclear Hartmann-Hahn (HOHAHA),<sup>16-19</sup> nuclear Overhauser effect (NOESY),<sup>20,21</sup> <sup>1</sup>H-<sup>13</sup>C heteronuclear multiple quantum coherence (HMQC),<sup>22-27</sup> <sup>1</sup>H-<sup>13</sup>C heteronuclear multiple-bond correlation (HMBC),<sup>28</sup> and double-quantum-filtered homonuclear-correlated (2QF-COSY)<sup>29</sup> spectroscopies. Using the approach developed in studies of coenzyme B<sub>12</sub>,<sup>11,12</sup> we have assigned completely the <sup>1</sup>H and <sup>13</sup>C NMR spectra of native F430 in TFE-*d*<sub>3</sub> and confirmed structural elements of F430 that were deduced from studies of F430M.

## Experimental Section

**Materials.** Phenyl-Sepharose CL-4B, QAE A-25, and DEAE-Sephadex A-25 were purchased from Pharmacia LKB Biotechnology Inc. C<sub>18</sub> reversed-phase HPLC columns (7.8 mm × 30 cm, 3.9 mm × 30 cm, and 3.9 mm × 15 cm) were purchased from Waters. PM30 ultrafiltration membranes (cutoff 30 000 Da) were obtained from Amicon. Deuterated trifluoroethanol was from Cambridge Isotopes.

**Bacterial Cells.** *Methanobacterium thermoautotrophicum* strain ΔH (DSM 1053) was grown in a 250-L fermentor (Braun) at 60 °C (pH 7.2) with H<sub>2</sub> and CO<sub>2</sub> as energy and carbon sources, respectively. Cells were harvested aerobically at the end of exponential growth (optical density ca. 3.0 at 660 nm) with a Sharples centrifuge. Cells were stored under N<sub>2</sub> at -20 °C as either a cell paste or a cell suspension of whole cells in 50 mM potassium phosphate (pH 7.0) buffer (1:1).

(8) Pfaltz, A.; Jaun, B.; Faessler, A.; Eschenmoser, A.; Jaenchen, R.; Gilles, H. H.; Diekert, G.; Thauer, R. K. *Helv. Chim. Acta* **1982**, *65*, 828.

(9) Livingston, D. A.; Pfaltz, A.; Schreiber, J.; Eschenmoser, A.; Ankel-Fuchs, D.; Moll, J.; Jaenchen, R.; Thauer, R. K. *Helv. Chim. Acta* **1984**, *67*, 334.

(10) Pfaltz, A.; Livingston, D. A.; Jaun, B.; Diekert, G.; Thauer, R. K.; Eschenmoser, A. *Helv. Chim. Acta* **1985**, *68*, 1338.

(11) Summers, M. F.; Marzilli, L. G.; Bax, A. J. *Am. Chem. Soc.* **1986**, *108*, 4285.

(12) Bax, A.; Marzilli, L. G.; Summers, M. F. *J. Am. Chem. Soc.* **1987**, *109*, 566.

(13) Pagano, T. G.; Yohannes, P. G.; Hay, B. P.; Scott, J. R.; Finke, R. G.; Marzilli, L. G. *J. Am. Chem. Soc.* **1989**, *111*, 1484.

(14) For examples see: Wuthrich, K. *Science* **1989**, *243*, 45. Clore, G. M.; Gronenborn, A. M. *CRC Crit. Rev. Biochem.* **1989**, in press.

(15) Summers, M. F.; South, T. L.; Hare, D. *Biochemistry* **1990**, in press.

(16) Braunschweiler, L.; Ernst, R. R. *J. Magn. Reson.* **1983**, *53*, 521.

(17) Davis, D. G.; Bax, A. *J. Am. Chem. Soc.* **1985**, *107*, 2820.

(18) Davis, D. G.; Bax, A. *J. Am. Chem. Soc.* **1985**, *107*, 7197.

(19) Bax, A.; Davis, D. G. In *Advanced Magnetic Resonance Techniques in Systems of High Molecular Complexity*; Nicolai, N., Valensin, G., Eds.; Birkhauser: Boston, 1986; p 21.

(20) Jeener, J.; Meier, B. H.; Bachmann, P.; Ernst, R. R. *J. Chem. Phys.* **1979**, *79*, 4546.

(21) Macura, S.; Ernst, R. R. *Mol. Phys.* **1980**, *41*, 1980.

(22) Muller, L. *J. Am. Chem. Soc.* **1979**, *101*, 4481.

(23) Bax, A.; Griffey, R. G.; Hawkins, B. L. *J. Am. Chem. Soc.* **1983**, *105*, 7188.

(24) Bax, A.; Griffey, R. G.; Hawkins, B. L. *J. Magn. Reson.* **1983**, *55*, 301.

(25) Live, D. H.; Davis, D. G.; Agosta, W. C.; Cowburn, D. *J. Am. Chem. Soc.* **1984**, *106*, 6104.

(26) Bendall, M. R.; Pegg, D. T.; Doddrell, D. M. *J. Magn. Reson.* **1983**, *52*, 81.

(27) Bax, A.; Subramanian, S. *J. Magn. Reson.* **1986**, *67*, 565.

(28) Bax, A.; Summers, M. F. *J. Am. Chem. Soc.* **1986**, *108*, 2093.

(29) Rance, M.; Sorensen, O. W.; Bodenhausen, B.; Wagner, G.; Ernst, R. R.; Wuthrich, K. *Biochem. Biophys. Res. Commun.* **1983**, *117*, 479.

**Isolation and Purification of F430.** Cells were broken anaerobically by passage through a French pressure cell at 15 000 psi. (All of the following steps were performed aerobically and at 5 °C.) DNase and RNase (Sigma) were added to the suspension to degrade nucleic acids. The broken cells were then centrifuged at 25000g (1 h) to remove cellular debris and unlysed cells. Ammonium sulfate was slowly added while the solution was stirred to reach a final concentration of 80% saturation.<sup>30</sup> This slurry was centrifuged for 3 h at 25000g. The supernatant contained component C, the methyl-CoM reductase enzyme, with bound native F430. Ultrafiltration with a PM30 membrane was used to desalt the protein. The retentate of ultrafiltration was applied to a phenyl-Sepharose CL-4B column (2.6 cm × 30 cm). The pass-through was collected with 2 M potassium acetate in 25 mM potassium phosphate buffer. Purity was determined with native gel electrophoresis (Phast System, Pharmacia). The methyl-CoM reductase was lyophilized overnight to remove H<sub>2</sub>O. F430 was extracted from the enzyme by resuspending the methyl-CoM reductase in 2 M lithium chloride in 80% ethanol.<sup>9</sup> The solution was stirred overnight at 5 °C and then centrifuged at 25000g to remove the denatured enzyme. The supernatant contained F430. The ionic strength of the supernatant was decreased to less than 0.1 M (with H<sub>2</sub>O), and the supernatant was applied to a QAE A-25 column (1.5 cm × 40 cm) previously equilibrated with 0.1 M NH<sub>4</sub>CO<sub>2</sub>H (pH 4.0). Under these conditions, F430 binds to the top of the column.<sup>31</sup> The column was washed with four bed volumes of H<sub>2</sub>O, and the F430 was eluted with 0.5 M NH<sub>4</sub>CO<sub>2</sub>H (pH 4.0; flow rate, 23 mL/h). This step removed the LiCl and ethanol and also concentrated the F430. The concentrated F430 was lyophilized overnight.

Finally, the F430 was purified with a Waters C<sub>18</sub> μBondapak column (3.9 mm × 15 cm). The F430 was resuspended into a minimal amount of 0.5 M NH<sub>4</sub>CO<sub>2</sub>H (pH 4.0) and injected onto a HPLC column with HPLC system I. HPLC system I: Waters C<sub>18</sub> μBondapak 3.9 mm × 15 cm; 13-min linear gradient; 100% H<sub>2</sub>O to 30% MeOH; 1 mL/min. The eluate was monitored at 214 and 431 nm. The symmetrical peak at 14.0 min (*N* = 1394) was collected. This system removed small amounts of contaminating diepimer and monoepimer F430 (see below). Purity was checked by reinjecting the purified F430 into HPLC system II. HPLC system II: Waters C<sub>18</sub> μBondapak 3.9 mm × 30 cm; 14-min linear gradient; 10% MeOH (in 50 mM NH<sub>4</sub>CO<sub>2</sub>H, pH 7.0) to 60% MeOH (50 mM NH<sub>4</sub>CO<sub>2</sub>H, pH 7.0); 1 mL/min. Once again, the peak appeared to be symmetrical and had a *t*<sub>R</sub> = 5.85 min (*N* = 453).

In order to assess the stereochemistry of our purified native F430, we purified the native form as well as the 12,13-diepimer and 13-monoepimer using column chromatography (DEAE A-25) as described.<sup>31</sup> These stereoisomers of F430 can be found unbound to the methyl-CoM reductase (i.e., "free") in the cytosol.<sup>32</sup> HPLC system III was developed to confirm the stereochemical purity of native F430. HPLC system III: Waters C<sub>18</sub> μBondapak column 7.8 mm × 30 cm; 20-min linear gradient; 50 mM NH<sub>4</sub>CO<sub>2</sub>H (pH 7.0) to 60% MeOH (50 mM NH<sub>4</sub>CO<sub>2</sub>H, pH 7.0); 1.5 mL/min. The eluent was monitored at 214 and 430 nm.

The retention times of the F430 stereoisomers were as follows: native F430, 13.0 min (*N* = 16 700); 12,13-diepimer, 13.9 min (*N* = 19 300); 13-monoepimer, 14.9 min (*N* = 22 000). The native F430 purified from the methyl-CoM reductase had the same retention time as the "free" native F430 purified from the cytosol. Both samples gave identical mass spectra (see below).

Two additional HPLC systems were developed to check for contamination due to factor F560 (12,13-didehydro-F430). This analogue of F430 has a major absorption at 560 nm and is purple, presumably due to an extended ring conjugation (through ring C).<sup>10</sup> The eluent was monitored at both 560 and 430 nm with HPLC systems IV and V. HPLC system IV: Waters C<sub>18</sub> μBondapak 3.9 mm × 30 cm; 25-min linear gradient; 10% MeOH (50 mM NH<sub>4</sub>CO<sub>2</sub>H, pH 7.0) to 50% MeOH (50 mM NH<sub>4</sub>CO<sub>2</sub>H, pH 7.0); 0.5 mL/min. The retention time of F560 was 17.0 min (*N* = 12 800). HPLC system V: Waters C<sub>18</sub> μBondapak 7.8 mm × 30 cm; 20-min linear gradient; 10% MeOH (50 mM NH<sub>4</sub>CO<sub>2</sub>H, pH 7.0) to 60% MeOH (50 mM NH<sub>4</sub>CO<sub>2</sub>H, pH 7.0); 1 mL/min. The retention times were 17.6 min for native F430 (*N* = 3500) and 19.2 min for F560 (*N* = 2050).

Optical spectra were also used to distinguish between the stereoisomeric forms of F430.<sup>10,31</sup> Spectra obtained for native F430 extracted from methyl-CoM reductase did not exhibit shoulders at 340 or 300 nm (unlike the diepimer). The absorbance ratio *A*<sub>430</sub>/*A*<sub>275</sub> was 1.05, matching published values for native F430,<sup>31</sup> and the half-height width of the 430 nm peak was 62 nm.

(30) Hartzell, P. L.; Wolfe, R. S. *Proc. Natl. Acad. Sci. U.S.A.* **1986**, *83*, 6726.

(31) Shiemke, A.; Hamilton, C.; Scott, R. *J. Biol. Chem.* **1988**, *263*, 801.

(32) Hausinger, R. P.; Orme-Johnson, W. H.; Walsh, C. T. *Biochemistry* **1984**, *23*, 801.

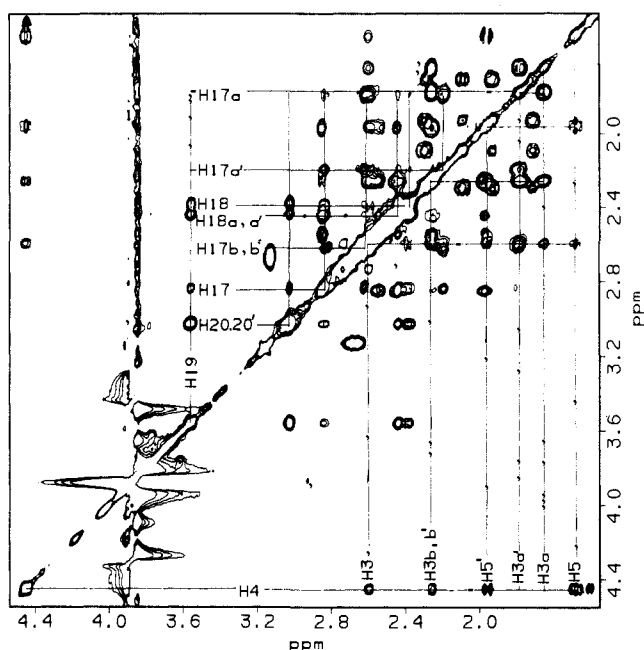


**Figure 1.** Portion of the 2D HOHAHA spectrum of native F430 showing connectivities for two independent  $J$ -networks. Weak cross peaks from H19 to H17a, H17a', and H17b,b' and from H4 to H3a and H3a' are visible at lower contour levels (see supplementary Figure S2).

On the basis of HPLC and UV-vis spectrophotometric analyses in aqueous solution, the native F430 samples were free of F560, 13-monopimer, and 12,13-diepimer contamination and were completely consistent with published UV-vis spectra. FAB cation mass spectrometry of native F430 gave an expected peak at  $m/z = 905$  (matrix nitrobenzyl alcohol).

The UV-vis spectrum of native F430 was substantially different in TFE solution (supplementary material) as should be expected on changing the electronic state of nickel(II) from predominantly high spin (aqueous) to predominantly low spin (TFE). However, dissolution of a small portion of the F430 NMR sample (TFE- $d_3$  solution) into  $H_2O$  (100-fold dilution) subsequent to NMR measurements gave the normal UV-vis spectrum expected for native F430 in aqueous solution (supplementary material).

**NMR Data.** NMR spectral data (500.14 MHz,  $^1H$ ) were obtained with a GE GN-500 spectrometer. Sample conditions were as follows: 5.1 mM native F430 in  $F_3CCD_2OD$  (TFE) solvent;  $T = 20^\circ C$ . Raw NMR data were transferred via ethernet to VAX and Silicon Graphics Personal Iris computers, converted to "readable" files with an in-house program (GENET), and processed with FTNMR (Hare Research, Inc.).  $^1H$  and  $^{13}C$  chemical shifts were referenced to internal TFE (3.88 ppm,  $^1H$ ; 61.5 ppm,  $^{13}C$ ).

Homocorrelated spectra were zero-filled to final matrix sizes of  $1024 \times 1024$  real points. Data acquisition and processing parameters for individual 2D experiments (defined below) were as follows. **2QF-COSY:** 96 scans per  $t_1$  increment; 2.8-s repetition delay;  $2 \times 256 \times 1024$  raw data matrix size, processed with 4-Hz Gaussian filtering in the  $t_2$  dimension and 8-Hz Gaussian plus trapezoidal filtering in the  $t_1$  dimension. **HOHAHA:**  $2 \times 256 \times 1024$  raw data matrix size; 32 scans per  $t_1$  increment; 2.8-s repetition delay; 60-ms MLEV-17 mixing period, preceded and followed by 2.5-ms trim pulses; 7.9-kHz spin lock field, corresponding to 32- $\mu s$   $90^\circ$  pulse widths; 6-Hz Gaussian and  $90^\circ$  shifted squared sine bell filtering in the  $t_2$  and  $t_1$  dimensions, respectively. **ROESY:**  $2 \times 256 \times 1024$  raw data matrix size; 64 scans per  $t_1$  increment; 2.4-s repetition delay; 85-ms continuous wave spin lock period; 6.25-kHz spin lock field strength, corresponding to 40- $\mu s$   $90^\circ$  pulse widths; 6-Hz Gaussian and  $90^\circ$  shifted squared sine bell filtering in the  $t_2$  and  $t_1$  domains, respectively. **NOESY:**  $2 \times 256 \times 1024$  raw data matrix size; 64 scans per  $t_1$  increment; 2.8-s repetition delay period; 400-ms mixing period; 6-Hz Gaussian and  $90^\circ$  shifted squared sine bell filtering in the  $t_2$  and  $t_1$  domains, respectively.  **$^1H$ - $^{13}C$  HMQC:**  $2 \times 128 \times 1024$  raw data matrix size; 128 scans per  $t_1$  increment; 1.2-s repetition delay period; 33- $\mu s$   $90^\circ$   $^{13}C$  pulse widths; 16 W of broad-band Waltz-16  $^{13}C$  decoupling during the acquisition period; 3.5-ms defocusing/refocusing delay periods; 800-ms "Weft" period; 6-Hz Gaussian and  $90^\circ$  shifted squared sine bell filtering in the  $t_2$  and  $t_1$  domains, respectively.  **$^1H$ - $^{13}C$  HMBC:**  $1 \times 200 \times 1024$  data matrix size; 512 scans per  $t_1$  increment; 2.0-s repetition delay; 33- $\mu s$   $90^\circ$   $^{13}C$  pulse widths; 3.5-ms

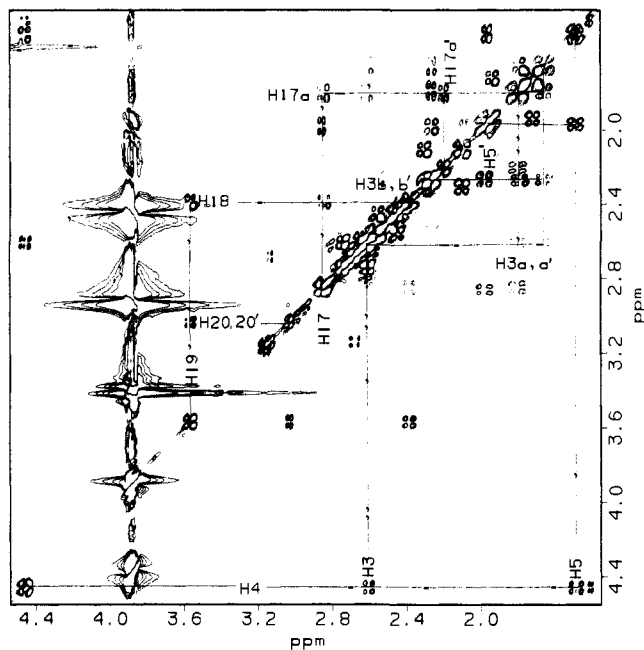


**Figure 2.** Portion of the 2D 2QF-COSY spectrum of native F430 with positive and negative contour levels drawn. Direct scalar connectivities are labeled for the same  $J$ -networks shown in Figure 1.

delay period for suppression of one-bond signals; 40-ms delay periods for long-range couplings;  $15^\circ$  shifted squared sine bell filtering in the  $t_2$  domain and no filtering in the  $t_1$  domain.

### NMR Methods and Spectra

The procedure used to assign the  $^1H$  and  $^{13}C$  NMR signals was similar to that developed for coenzyme  $B_{12}$ .<sup>11,12</sup> Initially,  $^1H$  signals were grouped into  $J$ -networks (networks of scalar coupled protons) with a HOHAHA spectrum obtained with a relatively long (64-ms) mixing period, Figure 1. The HOHAHA experiment is similar to the 2QF-COSY experiment (below) in that it provides through-bond, scalar connectivity information. However, the COSY data reveal only direct scalar coupling whereas the HOHAHA spectra contain direct and relayed  $J$ -coupling information. During the HOHAHA mixing period, magnetization is transferred from one proton (A) to a directly coupled proton (M) at a rate proportional to the  $J_{AM}$  coupling constant. If proton M is coupled to a third proton (X), magnetization can be relayed to X via the M proton. For longer mixing times, magnetization may be relayed to most or all protons within the same  $J$ -network. Direct scalar connectivities within a  $J$ -network are established from a COSY spectrum as shown in Figure 2.

Proton-carbon connectivities are then made with two types of  $^1H$ -detected heteronuclear multiple quantum NMR experiments. One-bond ( $^1J$ ) connectivities are made with the "BIRD-modified" HMQC pulse sequence, and multiple-bond ( $^2J$ ,  $^3J$ ) connectivities are established with HMBC spectroscopy. The  $^1J$  HMQC method is extremely useful for assigning geminal proton signals since both  $^1H$  signals correlate with a single-carbon frequency as shown in Figure 3. Although the  $^1J$ -HMQC experiment is very sensitive (data for Figure 3 were obtained in ca. 2.5 h), relatively rapid proton  $T_2$  relaxation decreased substantially the sensitivity of the HMBC experiment; the HMBC spectrum shown in Figure 4, obtained with a relatively short (40-ms) pulse-delay period, required ca. 60 h of data sampling.

Through-space  $^1H$ - $^1H$  dipolar interactions used to make inter- $J$ -network connectivities and stereochemical assignments were established with 2D NOESY and ROESY (rotating frame Overhauser effect)<sup>33-35</sup> NMR spectroscopies. A portion of the NOESY spectrum (400-ms mixing time) obtained for F430 is

(33) Bothner-By, A.; Stephens, R. L.; Lee, J. T.; Warren, C. D.; Jeanloz, R. W. *J. Am. Chem. Soc.* **1984**, *106*, 811.

(34) Davis, D.; Bax, A. *J. Magn. Reson.* **1985**, *63*, 207.

(35) Bax, A.; Sklenar, V.; Summers, M. F. *J. Magn. Reson.* **1986**, *70*, 327.

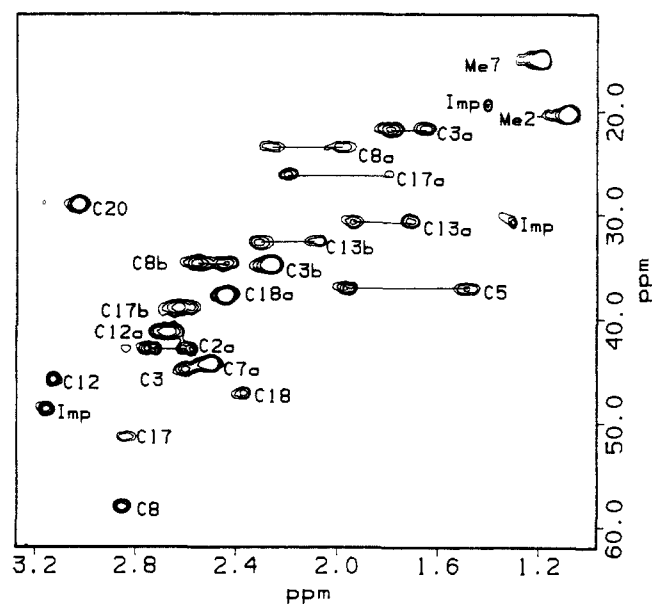


Figure 3. Portion of the 2D  $^1\text{H}$ - $^{13}\text{C}$  HMQC spectrum of native F430. Horizontal lines connect signals of geminal protons (Imp = impurity).

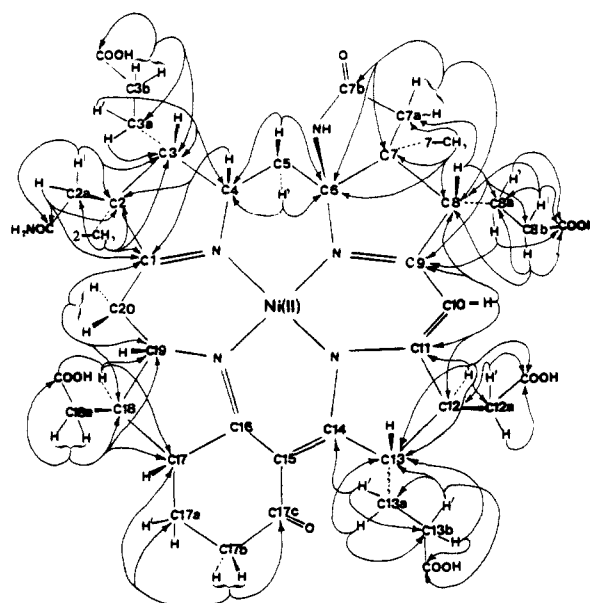


Figure 5. Summary of the two- and three-bond  $^1\text{H}$ - $^{13}\text{C}$  HMBC connectivities observed for native coenzyme F430.

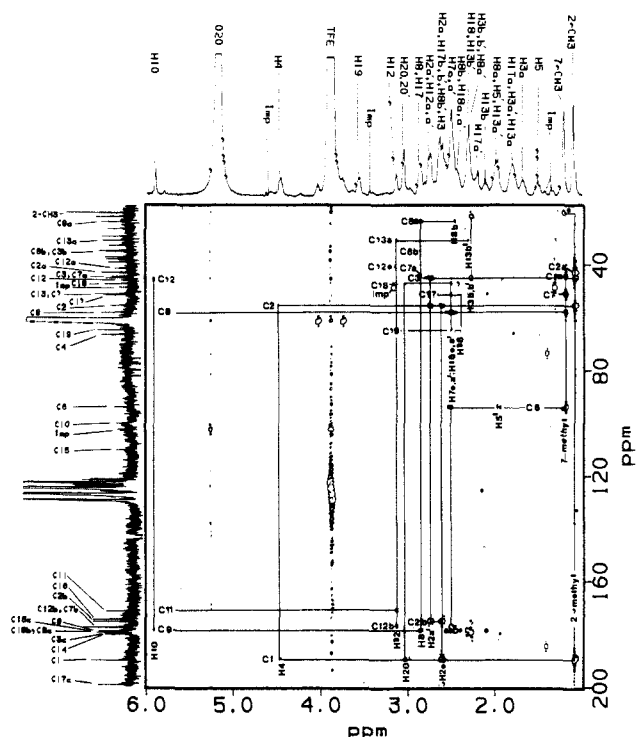


Figure 4. Portion of the 2D HMBC spectrum of native F430 showing two- and three-bond scalar connectivities used to assign carbon signals and establish (confirm) the covalent structure. Signals labeled with an asterisk and Imp are due to incompletely suppressed one-bond coherences and sample impurities, respectively. Columns associated with the water and TFE  $^1\text{H}$  frequencies are displayed at higher contour levels (3-fold) compared with the rest of the spectrum. Some of the  $^{13}\text{C}$  signals in the 1D spectrum have been labeled; see Table II for a complete list of assignments.

shown in Figure 6. ROESY spectroscopy is particularly useful for identifying spin diffusion cross peaks that have phases opposite to the phases of direct Overhauser effect cross peaks. At our field strength (11.75 T), ROESY cross peaks are also generally more intense than NOESY cross peaks due to the fact that the molecular tumbling time constant ( $\tau_c$ ) is approximately the same as the angular Larmor frequency ( $\omega_L$ ). However, the relatively small  $^1\text{H}$  NMR chemical shift dispersion for F430 resulted in significant Hartmann-Hahn transfer for many strongly coupled protons, complicating interpretation of the ROESY spectra. We therefore

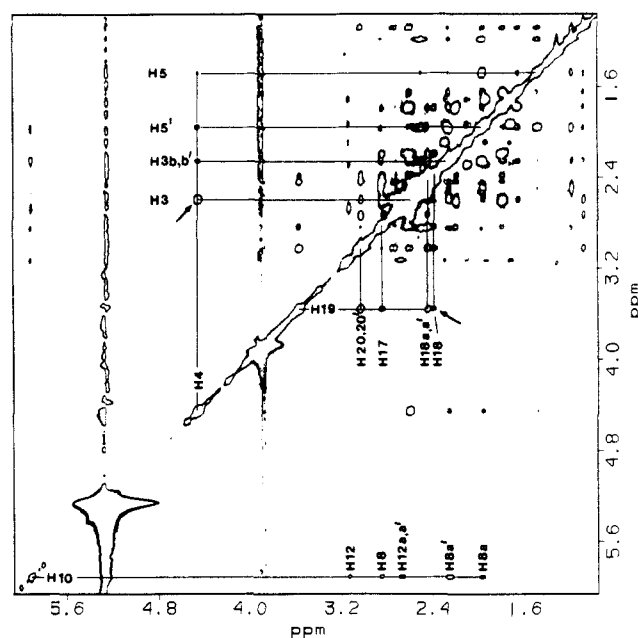


Figure 6. 2D NOESY spectrum obtained for native F430 in TFE solution with a mixing time of 400 ms. Arrows point to cross peaks used to assign the relative stereochemistry at C17 (see text).

used ROESY data only to evaluate for spin diffusion for non-coupled protons (data not shown).

#### Signal Assignments

Two independent  $J$ -networks are illustrated and labeled in a portion of the HOHAHA spectrum shown in Figure 1. The  $^1\text{H}$  NMR signal at 4.45 ppm in the HOHAHA spectrum gives strong cross peaks to signals at 2.60, 2.26, 1.95, and 1.48 ppm (see Figure 1) and weaker cross peaks to signals at 1.77 and 1.65 ppm (observed at lower contour levels; see supplementary figures). These signals comprise a single  $J$ -network. The 4.45 ppm signal gives direct scalar connectivity with signals at 2.60 and 1.48 ppm (see 2QF-COSY spectrum, Figure 2).

Examination of the  $^1\text{H}$ - $^{13}\text{C}$  HMQC spectrum (Figure 3) reveals that the 2.60 ppm signal is due to a methine proton (i.e., this is the only proton signal that correlates with the carbon signal at 44.9 ppm), whereas the 1.48 ppm proton signal results from one of two geminal protons that correlates with the carbon signal at 37.0 ppm. The remaining geminal proton signal occurs at 1.95

Table I. Scalar and Dipolar NMR Connectivities Used To Assign  $^1\text{H}$  and  $^{13}\text{C}$  Signals in Native Coenzyme F430<sup>a</sup>

$^1\text{H}$ signal	HOHAHA	COSY	NOESY	HMBC
Me2			H2a (s), H2a' (s), H3 (s), H3a (w), H3a' (w), H3b (w), H3b' (w), H5 (s), H5' (w), H20 (s)	C1, C2, C2a, C3
Me7			H5 (s), H5' (s), H7a,a' (s), H3b (s), H3b' (s), H8 (w), H8b,b' (s), H8a (overlaps with H5' signal), H8a'	C6, C7, C7a, C8
H2a	H2a'	H2a'	H2a' (s), H-Me2 (s)	C2b, C2, C1
H2a'	H2a	H2a	H2a (s), H-Me2 (s) H18a,a' (w)	C2b, C2, C3
H3	H3a, H3a', H3b,b', H5, H5'	H3a, H3a' (overlaps with H17a)	H-Me2 (s), H3a (m), H3a' (m), H3b,b' (s), H5' (m), H4 (s)	C1
H3a	H3b, H3b', H4	H3a'	H5 (w), H-Me2 (m)	C3
H3a'	H3b, H3b', H4	H3a	H-Me2 (m), H3a (s), H5 (w)	C3b
H3b,b'	H3b, H3b', H5	H3a, H3a'	H3a (m), H3a' (m), H5 (w), H5' (s)	C3a, C3, C3c
H4	H3, H3a, H3a', H3b,b', H5, H5'	H3, H5	H3 (s), H3b,b' (m), H5 (w), H5' (w)	C2, C1
H5	H5'	H5'	H-Me2 (m), H-Me7 (s)	C4, C6
H5'	H5	H5	H-Me2 (m), H-Me7 (s), H3a,a' (m), H5 (s)	C4, C6
H7a,a'	H8a, H8a'		H5 (w), H5' (m), H-Me7 (s), H8a (w), H8a' (w)	C6, C7, C7b, C8
H8	H8a, H8a'	H8a	H7a,a' (s), H8a (m), H8a' (m), H8b (s), H8b' (w), H-Me7 (w)	C9, C7a, C8a, C8b
H8a	H8, H8a', H8b,b'	H8a'	H5 (s), H10 (m), H-Me7 (s)	C9, C8c
H8a'	H8, H8a, H8b,b'	H8a	H-Me7 (s), H8a (s)	C8c
H8b	H8a, H8a', H8b'	H8a	H8a (w), H8a' (m)	C8a, C8c, C8
H8b'	H8a, H8a', H8b	H8a	H8a (w), H8a' (m)	C8a, C8c, C8
H10	none	none	H8 (m), H8a (m), H8a' (s), H12 (m), H12a,a' (m)	C8, C9, C11, C12
H12	H12a,a', H13a H13a', H13b, H13b'	H12a,a'	H12a,a' (s), H13a (w) H13a' (w), H13b (w), H13b' (w)	C13, C11, C12b, C12a, C13a C12, <sup>b</sup> C12b
H12a,a'	none	none		
H13	H13a, H13a', H13b, H13b', H12, H12a,a'	c	c	c
H13a	H13b, H13b', H13a'		H13a' (w), H13b' (w)	C13b, C13, C13b, C14
H13a'	H13b, H13b', H13a			C13c, C13
H13b	H13a, H13a', H13b'	H13b', H13a'	H13a (w), H13a' (w)	C13a, C13c, C13
H13b'	H13a, H13a', H13b	H13b	H13a (w), H13a' (w), H13b (s)	
H17	H17a, H17a', H17b,b', H18, H18a,a'		H17a (w), H17a' (m), H17b,b' (m), H18 (m), H18a,a' (s)	
H17a	H17, H17a', H17b, H17b,b'	H17a'	H17a' (s)	
H17a'	H17, H17a, H17b, H17b,b', H18, H18a, H18a,a'	H17a	H17a (s)	
H17b,b'	H17a, H17a'		H17a (s), H17a' (s), H18a,a' (w)	C17, C17a, C17c
H18	H17a, H17a'	none	H17a (m), H17a' (m)	C19, C18b, C17
H18a,a'	H17a, H17a', H18		H17a (m), H17a' (m)	C17, C18, C18b, C19
H19	H17, H17a', H18, H18a,a', H20,20', H17b,b'	H20,20', H18	H17 (m), H18 (m), H18a,a' (s), H20,20' (s)	
H20,20'	H17, H18, H18a,a'	H19	H-Me2 (s), H2a' (s), H17 (w), H18 (s), H18a,a' (s), H2a (s)	C1, C19, C18

<sup>a</sup> Primes refer to the downfield signal for resolved geminal proton pairs. s, m, and w refer to strong, medium, and weak NOESY cross-peak intensities, respectively. <sup>b</sup> Tentative, based on a weak correlation peak in the 2D spectrum. <sup>c</sup> Correlation signals not observed due to rapid substitution of deuterium for H13.

ppm in the  $^1\text{H}$ - $^{13}\text{C}$  HMQC spectrum, consistent with 1.95 ppm cross peak observed in the HOHAHA spectrum described above. As expected for geminal protons, a strong cross peak is observed in the 2QF-COSY spectrum for the proton signals at 1.48 and 1.95 ppm (see Figure 2). In addition, the 2.60 ppm methine proton exhibits direct scalar coupling to the *J*-network signals at 1.77 and 1.65 ppm (Figure 2), which are also geminal protons (see Figure 3). Finally, the 1.77 and 1.65 ppm signals give 2QF-COSY cross peaks with the signal at 2.26 ppm (Figure 2), which has an integrated intensity of two protons (see Figure 3). This *J*-network pattern is consistent only with protons at positions 3-5 in F430 and is assigned as indicated in Figures 1-3.

When the 2QF-COSY, HOHAHA, and  $^1\text{H}$ - $^{13}\text{C}$  HMQC spectra are compared as described above, signals for nearly all of the protons (and their directly attached carbons) could be assigned specifically. Due to relatively rapid exchange of H13 for deuterium in TFE solution (apparent  $t_{1/2}$  on the order of a few hours), correlations with H13 were only observed in spectra obtained for freshly prepared samples (e.g., see supplementary HOHAHA spectrum). In addition, signals due to protons and carbons at the 2a- and 7a-positions could not be uniquely identified with the  $^1\text{H}$ - $^1\text{H}$  scalar-correlated data alone since their respective *J*-network patterns are identical (the H2a, H2a' and H7a, H7a' geminal protons do not exhibit further scalar coupling). However,

one set of protons (H7a,a') exhibited a strong NOE with the Me7 protons, whereas the other set of geminal protons (H2a,a') gave a strong NOE with the Me2 protons (Table I), enabling unambiguous assignment of  $^1\text{H}$  and  $^{13}\text{C}$  signals for atoms at positions 2a and 7a.

Assignments for carbons without attached protons were then made with  $^1\text{H}$ - $^{13}\text{C}$  HMBC spectroscopy, which also provided a means of confirming  $^1\text{H}$  and  $^{13}\text{C}$  signal assignments made above. A portion of the HMBC spectrum obtained for F430 is shown in Figure 4, and expansions are given in the supplementary material. In Figure 4, HMBC correlation signals are observed from the H10 proton signal to carbon signals at 58.5 and 46.3 ppm. These signals are assigned to the C8 and C12 carbons on the basis of one-bond  $^1\text{H}$ - $^{13}\text{C}$  HMQC correlations (above). Two remaining HMBC signals from H10 at 179.3 and 171.8 ppm must be due to correlations with the C9 and C11 carbons. Specific assignment of these signals to C9 (179.3) and C11 (171.8) is possible since the H8 signal correlates with C9 whereas the H12 signal correlates with C11 (Figure 4). All of the HMBC correlations are summarized in Table I and are illustrated by arrows in Figure 5. The C15 and C16 carbons could not be assigned on the basis of HMBC connectivities. Since only two signals at 174.8 and 110.4 ppm remained to be assigned in the  $^{13}\text{C}$  spectrum (Figure 5), these signals were assigned to C16 and C15, respectively, on the basis

Table II. <sup>13</sup>C NMR Signal Assignments for Native Coenzyme F430<sup>a</sup>

signal assgnt		native F430	
present	(prev <sup>b</sup> )	present	(prev <sup>b</sup> )
C17c	(C17c)	199.6	(199.5)
C1	(C1)	190.3	(190.2)
C14	(C14 or C16)	180.5	(180.5)
C3c	(C9)	180.2	(180.3)
C18b	c	179.7	(179.8)
C8c	c	179.7	(179.6)
C13c	c	179.5	(179.6)
C9	c	179.3	(179.3)
C12b	c	177.8	(177.9)
C7b	c	177.8	(177.7)
C2b	c	175.6	(175.6)
C16	c	174.8	(174.7)
C11	(C11)	171.8	(171.7)
C15	(C15)	110.4	(110.4)
C10	(C10)	100.3	(100.3)
C6	(C6)	94.1	(94.2)
C4	(C4)	66.9	(66.9)
C19	(C19)	65.2	(65.1)
C8	(C8)	58.5	(58.5)
C2	(C2)	55.9	(55.9)
C17	(C13)	51.8	(51.8)
C7	(C7)	51.5	(51.4)
C13	(C17)	51.5	(51.4)
C18	(C12 or C18)	47.6	(47.6)
C12	(C12 or C18)	46.3	(46.4)
C3	(C3)	45.4	(45.4)
C7a	(C2a or C7a)	44.8	(44.8)
C2a	(C2a or C7a)	43.3	(43.3)
C12a	(C12a or C17b)	41.7	(41.9)
C17b	(C12a or C17b)	39.3	(39.4)
C18a	(C5)	38.2	(38.1)
C5	(C18a)	37.5	(37.5)
C3b	(C3b or C8b or C13b)	35.2	(35.3)
C8b	(C3b or C8b or C13b)	35.1	(35.1)
C13b	(C3b or C8b or C13b)	33.0	(33.1)
C13a	(C13a)	31.1	(31.1)
C20	(C20)	29.5	(29.5)
C17a	(C3a or C8a or C17a)	26.6	(26.6)
C8a	(C3a or C8a or C17a)	24.0	(23.9)
C3a	(C3a or C8a or C17a)	22.1	(22.1)
Me2	(Me2)	20.6	(20.6)
Me7	(Me7)	15.5	(15.5)

<sup>a</sup> Results for samples in TFE-*d*<sub>3</sub>. <sup>b</sup> Reference 9. <sup>c</sup> Not assigned previously.

of expected chemical shifts. Complete <sup>13</sup>C and <sup>1</sup>H NMR chemical shift assignments are summarized in Tables II and III, respectively.

### Conformational Analysis

1D NOE data were used in previous studies of F430M to make stereochemical assignments for all but one chiral carbon of the corphin macrocycle. Except for some differences in the classification of NOE intensities (strong (s), medium (m), weak (w)), signals observed here in the 2D NOESY spectrum of native F430 (Figure 6; Table I) are consistent with NOEs observed for F430M. For example, the 2D NOESY spectrum of native F430 exhibited cross peaks from Me2 to H20,20' (s), H2a,a' (s), H3a,a' (m), H3b,b' (w), and H5 (m) protons; from H4 to H3 (s) and H5,5' (w); from H5' to Me7 (s) and Me2 (m); from H5 to Me7 (m); from Me7 to H8 (w), H8a' (m), and H8b,b' (w); from H8 to H10 (m); from H10 to H12 (m) and H12a,a' (m); and from H12 to H13a,a' (w) and H13b,b' (w). These data are consistent with the 1D NOE data reported for F430M and are also consistent with the previous NOE-derived stereochemical assignments.

In addition to corroborating earlier NOE-derived stereochemical assignments, the stereochemistry of carbon C17 was assigned as follows. H17 and H19 give approximately equal (moderate) NOEs to the H18a,a' protons (see Figure 6). In addition, H17 gives only a weak NOE cross peak to H18, which is of approximately the same intensity as the H18-H19 cross peak. These data are consistent with the *R* stereochemical assignment for the C17 carbon as shown in Figure 5. Note that if the stereochemistry of C17 had been *S*, then H17 and H18 would have been *cis* to

Table III. <sup>1</sup>H NMR Signal Assignments for F430 and F430M<sup>a</sup>

assgnt	F430	F430M	assgnt	F430	F430M
Me2	1.08	1.11	H10	5.91	5.72
Me7	1.18	1.20	H12	3.13	3.12
H2a	2.60	2.64	H12a,a'	2.67	2.65
H2a'	2.73	2.78	H13	3.91	3.80
H3	2.60	2.68	H13a	1.71	1.70
H3a	1.65	1.58	H13a'	1.93	1.90
H3a'	1.77	1.76	H13b	2.09	2.13
H3b,b'	2.26	2.29	H13b'	2.29	2.30
H4	4.45	4.48	H17	2.83	2.63
H5	1.48	1.53	H17a	1.78	1.76
H5'	1.95	1.87	H17a'	2.19	2.11
H7a	2.49	2.43	H17b	2.58	<i>b</i>
H7a'	2.49	2.51	H17b'	2.63	<i>b</i>
H8	2.86	2.84	H18	2.38	2.50
H8a	1.98	1.96	H18a,a'	2.45	2.72
H8a'	2.26	2.22	H19	3.55	3.53
H8b	2.44	<i>b</i>	H20	3.02	2.98
H8b'	2.56	<i>b</i>	H20'	3.02	3.12

<sup>a</sup> Results for native F430 in TFE-*d*<sub>3</sub> solution from present work; results for F430M in CD<sub>2</sub>Cl<sub>2</sub> solution from ref 8. <sup>b</sup> Not assigned.

each other and a very strong NOE cross peak would be expected. The dramatic difference between the weak H17-H18 and very strong H3-H4 (*cis* protons) cross peaks is evident in the NOESY spectrum shown in Figure 6 (see arrows).

The above absolute stereochemical assignments for C17, C18, and C19 rely on the assumption that the original assignment of C19 (*S*) is correct. The original stereochemical assignment of C19 was made on the basis of the H19 chemical shift and the NOE interactions between the H20 and Me-2 protons, which might be considered tentative (A. Eschenmoser, B. Juan, A. Pfaltz, C. Kratky, personal communication). If the stereochemistry of C19 were actually *R*, then the stereochemistries of C18 and C17 would have to be *S* and *S*, respectively, on the basis of relative C19-H, C18-H, and C17-H NOE intensities. However, preliminary 2D NOESY back-calculations, which provide theoretical NOESY spectra for F430 models containing both possible stereochemistries, suggest strongly that the original assignment must be correct.<sup>36</sup> Complete details of these results and the new methodology will be published elsewhere.<sup>37</sup>

### Discussion

The <sup>13</sup>C NMR spectrum obtained for F430 in TFE-*d*<sub>3</sub> is virtually identical with the spectrum observed previously for a similar F430 sample,<sup>9</sup> with chemical shifts agreeing to within 0.2 ppm (Table II). Of the 21 specific <sup>13</sup>C signal assignments made earlier, only five carbon assignments (C9, C5, C18a, C13, C17) appear to have been made erroneously as indicated in Table II. As mentioned above, <sup>1</sup>H NMR chemical shifts and signal assignments were not reported previously for native F430 due to the presence of broad, unresolved signals in the 300-MHz NMR spectrum. However, for the 42 proton assignments reported for F430M in CD<sub>2</sub>Cl<sub>2</sub> solution, our assignments for native F430 are in good agreement (Table III).

In addition, by achieving higher spectral resolution at 500-MHz field strength and using 2D methods, we were able to assign the H8b, H8b', H17b, and H17b' proton signals that had not been assigned previously for F430M. The only <sup>1</sup>H signals not examined in the present study were those for the amide protons, which exchange rapidly with deuterium in TFE-*d*<sub>3</sub> solution. Although the H13 proton is also relatively labile in TFE-*d*<sub>3</sub>, deuterium incorporation was sufficiently slow to allow observation of the H13 proton signal in the HOHAHA spectrum obtained under rapid acquisition conditions.

The highly redundant set of <sup>1</sup>H-<sup>1</sup>H and <sup>1</sup>H-<sup>13</sup>C NMR connectivities (Table I and Figure 5) unambiguously confirms the covalent structure of F430 determined in earlier studies of F430M. The fact that nearly identical <sup>1</sup>H NMR chemical shifts were

(36) Based primarily on relative Me-2 to H19 NOE intensities.  
(37) Manuscript in preparation.

observed in these studies suggests that there are no major structural or electronic differences between F430 and F430M in TFE- $d_3$  and  $CD_2Cl_2$  solutions, respectively. Qualitative analyses of the 2D NOESY data are consistent with stereochemical assignments made previously for F430M with 1D NOE methods and are also consistent with an *R* stereochemistry assignment for the C17 carbon. However, additional experiments will be necessary to establish unambiguously whether the C17-C18-C19 stereochemical assignments are *R,R,S* or *S,S,R*, respectively. Although the  $^1H$  NMR signals exhibited by native F430 are relatively broad even at 500-MHz field strength, it is clearly possible to obtain detailed structural information and signal assignments from small sample quantities (2 mg) with the recently developed 2D NMR experiments. Having confirmed aspects of the covalent structure and completed the  $^1H$  NMR assignment, we have set the stage for determination of the 3D solution structure of native F430 to atomic level resolution using new 2D NOESY back-calculation and

distance geometry methods (underway).

**Acknowledgment.** Financial support from the Petroleum Research Fund, administered by the American Chemical Society (to M.F.S.), and the NSF (Grant 1-5-29812 NSF DMB 86-13679 to R.W.) and technical support from Victor Gabriel (UIUC), Scott Smith (UIUC), and Jack Suess (UMBC) are gratefully acknowledged.

Registry No. Coenzyme F430, 73145-13-8.

**Supplementary Material Available:** Expansions of 2D HOH-AHA spectra with labeled *J*-networks (Figure S1), 2D HOHAHA spectra at low contour levels (Figure S2), full 2D  $^1H$ - $^{13}C$  HMQC spectrum of F430 (Figure S3), portions of 2D HMBC spectrum for F430 (Figures S4 and S5), and UV-vis spectra of F430 in  $H_2O$  and TFE- $d_3$  (Figure S6) (6 pages). Ordering information is given on any current masthead page.

## Infrared Intensities: Bicyclo[1.1.0]butane. A Normal Coordinate Analysis and Comparison with Cyclopropane and [1.1.1]Propellane

Kenneth B. Wiberg,\* Sherman T. Waddell, and Robert E. Rosenberg

Contribution from the Department of Chemistry, Yale University, New Haven, Connecticut 06511.  
Received June 16, 1989

**Abstract:** The infrared and Raman spectra of bicyclo[1.1.0]butane and of its 1,3- $d_2$  and 2,2,4,4- $d_4$  isotopomers were redetermined, and the intensities of the infrared bands were measured. A new vibrational assignment was made with the help of the spectrum calculated by using the 6-31G\* basis set. A normal coordinate analysis was carried out, and the infrared intensities were converted to atomic polar tensors and to dipole moment derivatives with respect to symmetry coordinates. The results of this investigation are compared with the data for cyclopropane and for [1.1.1]propellane in order to determine the effect of the structural changes on the properties of the methylene groups of these molecules.

### I. Introduction

One of the goals of physical organic chemistry is to be able to describe structural and substituent effects in as detailed a fashion as possible. Molecular spectroscopy has the potential for providing such information. As an example, consider the methylene groups of cyclopropane (1), bicyclo[1.1.0]butane (2), and [1.1.1]propellane (3). If it were possible to determine the force constants for the vibrations of the methylene groups, along with the dipole moment derivatives for these vibrations, one would have a good description of how the group changes through the series.



We have presented a normal coordinate analysis for [1.1.1]propellane and have determined the dipole moment derivatives with respect to the symmetry coordinates.<sup>1</sup> Corresponding data for cyclopropane also are available.<sup>2</sup> We have reported a vibrational assignment and a normal coordinate analysis for bicyclobutane,<sup>3</sup> and another assignment has been reported by Aleksanyan et al.<sup>4</sup> However, they must be considered as first

approximations since many of the bands are quite weak and relatively difficult to assign. In addition, it now seems clear that a unique force field cannot be obtained for a polyatomic molecule by using only observed vibrational frequencies.<sup>5</sup> The off-diagonal elements of the force constant matrix are often coupled to the diagonal terms so that changes in one may be compensated by changes in the other without significantly changing the calculated frequencies. Therefore, we have reinvestigated the vibrational spectrum of 2 with the aid of theoretical calculations, and in addition, we have measured the intensities of the infrared bands so that the changes in dipole moment resulting from molecular distortions could be determined.

### II. Vibrational Spectrum of Bicyclobutane

The two main problems with bicyclobutane are those of making a satisfactory vibrational assignment for the weaker bands in the spectrum and of finding a unique solution to the normal coordinate problem. A calculation of the vibrational spectrum with ab initio MO theory provides useful information.<sup>6</sup> First, after appropriate scaling, the calculated frequencies and intensities are a good guide to what should be found for each symmetry block.<sup>7</sup> Second, the

(4) Aleksanyan, V. T.; Ezernitskaya, M. G.; Zotova, S. V.; Abramova, N. M. *Izv. Akad. Nauk. SSSR, Ser. Khim.* 1976, 1, 81.

(5) For an extreme example of multiple force fields see: Wiberg, K. B.; Dempsey, R. C.; Wendoloski, J. J. *J. Phys. Chem.* 1984, 88, 5596.

(6) Hess, B. A., Jr.; Schaad, L. J.; Carsky, P.; Zahradnik, R. *Chem. Rev.* 1986, 86, 709.

(1) Wiberg, K. B.; Dailey, W. P.; Walker, F. H.; Waddell, S. T.; Crocker, L. S.; Newton, M. D.; *J. Am. Chem. Soc.* 1985, 107, 7247.

(2) Kondo, S.; Nakanaga, T.; Saeki, S. *Spectrochim. Acta* 1979, 35A, 181.

(3) Wiberg, K. B.; Peters, K. S. *Spectrochim. Acta* 1977, 33A, 261.